DOI: 10.1002/JLB.2A0220-127R

JLB JOURNAL OF LEUKOCYTE BIOLOGY

ARTICLE

Role of endocytosis and trans-endocytosis in ICOS costimulator-induced downmodulation of the ICOS Ligand

Laura Aragoneses-Fenoll[1] | María Montes-Casado[1] | Gloria Ojeda[1] | Lucía García-Paredes[2,7] | Yutaka Arimura[3] | Junji Yagi[4] | Umberto Dianzani[5] | Pilar Portolés[1,6] | José M. Rojo[2]

[1]Unidad de Inmunología Celular, Centro Nacional de Microbiología, Instituto de Salud Carlos III, Majadahonda, Madrid 28220, Spain

[2]Departamento de Biomedicina Molecular, Centro de Investigaciones Biológicas Margarita Salas, CSIC, Madrid 28040, Spain

[3]Host Defense for Animals, Nippon Veterinary and Life Science University, 1-7-1 Kyonan, Musashino, Tokyo 180–8602, Japan

[4]Department of Microbiology and Immunology, Tokyo Women's Medical University, Tokyo 108–8639, Japan

[5]Interdisciplinary Research Center of Autoimmune Diseases (IRCAD) and Department of Health Sciences, University of Piemonte Orientale (UPO), Novara 28100, Italy

[6]Presidencia, Consejo Superior de Investigaciones Científicas, Madrid 28006, Spain

[7]Current address: Hospital 12 de Octubre, Departamento de Oncología Médica, Av. de Córdoba, s/n, Madrid, 28041, Spain

Correspondence
Pilar Portolés, Unidad de Inmunología Celular, Centro Nacional de Microbiología, Instituto de Salud Carlos III, Ctra. Pozuelo-Majadahonda, km 2, E-28220 Majadahonda, Madrid, Spain
Email: pportols@isciii.es
Jose M. Rojo, Departamento de Biomedicina Molecular, Centro de Investigaciones Biológicas Margarita Salas, CSIC, Ramiro de Maeztu, 9, E-28040 Madrid, Spain.
Email: jmrojo@cib.csic.es

Abstract

The interaction between the T-lymphocyte costimulatory molecule ICOS and its ligand (ICOS-L) is needed for efficient immune responses, but expression levels are tightly controlled, as altered expression of ICOS or ICOS-L may lead to immunodeficiency, or favor autoimmune diseases and tumor growth.

Using cells of mouse B cell lymphoma (M12.C3) and melanoma (B16), or hamster CHO cells transfected with various forms of mouse ICOS-L, and $ICOS^+$ T cell lines, we show that, within minutes, ICOS induces significant downmodulation of surface ICOS-L that is largely mediated by endocytosis and trans-endocytosis. So, after interaction with $ICOS^+$ cells, ICOS-L was found inside permeabilized cells, or in cell lysates, with significant transfer of ICOS from $ICOS^+$ T cells to ICOS-L-expressing cells, and simultaneous loss of surface ICOS by the T cells. Data from cells expressing ICOS-L mutants show that conserved, functionally important residues in the cytoplasmic domain of mouse ICOS-L (Arg_{300}, Ser_{307} and Tyr_{308}), or removal of ICOS-L cytoplasmic tail have minor effect on its internalization.

Internalization was dependent on temperature, and was partially dependent on actin polymerization, the GTPase dynamin, protein kinase C, or the integrity of lipid rafts. In fact, a fraction of ICOS-L was detected in lipid rafts. On the other hand, proteinase inhibitors had negligible effects on early modulation of ICOS-L from the cell surface.

Our data add a new mechanism of control of ICOS-L expression to the regulation of ICOS-dependent responses.

KEYWORDS

T Lymphocyte, Costimulation, ICOS, ICOS-L, Trans-endocytosis, Trogocytosis

Abbreviations: APC, Antigen-Presenting Cell(s); DC, Dendritic Cell; GFP, Green Fluorescent Protein; ICOS, Inducible Costimulator; ICOS-L, ICOS Ligand; ILC, Innate Lymphoid Cell(s); PMA, Phorbol Myristic acetate; Tfh, Follicular T helper cell; TMP, T cell Microvilli Particles.

Received: 6 March 2020 | Revised: 16 December 2020 | Accepted: 13 January 2020

1 | INTRODUCTION

Adaptive immune responses to pathogens or tumors are initiated by antigen recognition through antigen-specific receptors in the membrane of T and B lymphocytes. However, in addition to antigen receptor signals (signal 1), the development of efficient immune responses need additional signals delivered by interaction of costimulatory molecules in the membrane of lymphocytes and antigen-presenting cells (APC) (signal 2), plus signals induced by cytokines and chemokines (signal 3). Together, these signals induce the expansion of antigen-specific lymphocytes, their differentiation into effector and memory cells, and its adequate location to remove antigens.

The inducible costimulator (ICOS, H4, CD278) belongs to the CD28 family of regulators of immune responses.[1–3] This family includes costimulatory molecules that foster antigen activation of T lymphocytes (CD28, ICOS) as well as negative regulators of immune responses like CTLA-4, PD-1, or BTLA-4. Their ligands belong to the B7 family, so that CD28 and CTLA-4 bind B7-1 (CD80) and B7-2 (CD86), and ICOS binds the ICOS ligand (ICOS-L, B7h, CD275, GL50, B7RP-1, LICOS, B7-H2).

ICOS is characteristically expressed by activated T cells, where it serves as a costimulatory molecule promoting the differentiation of effector Th cells and enhancing the secretion of cytokines like IL-10, IL-17 and IFN-γ in humans, or IL-4 in mice.[4–7] Follicular helper CD4$^+$ T cells (Tfh) express the highest levels of ICOS, and ICOS is essential to the development of germinal centers, the cooperation with B cell activation, isotype switch, and maturation of normal or autoimmune antibody responses, so that ICOS deficiency is a cause of human immunodeficiency.[8–13] ICOS ligation also induces T cell motility[14–16] that contributes to germinal center formation.[17] Furthermore, ICOS signals promote the survival of effector memory and Treg CD4$^+$ T cells.[18,19] Last, recent data show the expression of and a role for ICOS in the function and/or survival of leukocytes other than T lymphocytes, including dendritic cells (DC)[20] or innate lymphoid cells (ILC).[21–23]

On the other hand, the ICOS-L is expressed by cells of hematopoietic and non-hematopoietic origin. These include professional APC (DC, macrophages and B lymphocytes), and a subset of T lymphocytes and ILC. Among non-hematopoietic cells, ICOS-L can be expressed by fibroblasts, epithelial cells and vascular endothelial cells, as well as various types of tumor cells and tumor cell lines.[7,24–31]

A prime function of ICOS-L is the induction of ICOS-mediated costimulatory signals in T cells during antigen responses "in vivo" and "in vitro[7,28,32–34]". Furthermore, ICOS-L expression by non-professional APC allows ICOS-mediated regulation of antigen activation, i.e. in experienced effector/memory T cells.[26,27]

In addition, ICOS-L itself delivers signals in ICOS-L expressing cells including DC, the prototypic professional APC. In mouse DC, ICOS-L signals induce interleukin 6 (IL-6), and enhance phagocytosis and antigen-presentation.[35] Our results in monocyte-derived human DC show that ICOS-L signalling enhanced LPS-induced secretion of cytokines IL-10 and IL-23, antigen cross-presentation by class I MHC, DC adhesion to endothelial cells, or chemokine-induced migration[36]; similar conclusions have been reached by Hedl et al.[20] Interaction with ICOS also inhibited the migration of ICOS-L$^+$ non-hematopoietic cells including endothelial cells and different types of tumor cells,[30,36] the adhesion between endothelial cells and polymorphonuclear leukocytes or tumor cell lines,[31] and osteoclast differentiation.[37]

The nature of ICOS-L-induced signals depends on the experimental system. So, whereas induction of IL-6 in mouse DC is dependent on the p38 MAPK,[35] ICOS-L lowers ERK activation induced by E-selectin or osteopontin.[31] ICOS-L signaling also inhibited focal adhesion kinase (FAK) tyrosine phosphorylation and induced lower levels of the Rac-1 activator β-Pix.[30,36] Last, ICOS-L enhancement of pattern recognition receptor (PRR) signals was dependent on the cytoplasmic tail of ICOS-L through recruitment and activation of the adaptor RACK1, and the kinases PKC and JNK.[20]

The expression levels of ICOS-L are essential to regulate its functions, and are subject to strict control. So, ICOS-L deficiency leads to major defects in immune responses,[13,34] and altered levels of ICOS-L in humans or mice have significant effects on the development of immune responses and autoimmune diseases.[7,20,38–43] In naïve B lymphocytes activated by IL-4 or BCR stimuli, ICOS-L is downmodulated within 24h through Ca^{++}- and STAT-6-mediated mechanisms.[44] This phenomenon involved the disappearance of ICOS-L mRNA, and could be blocked by CD40 signals.[44] In addition, the interaction with ICOS$^+$ cells or ICOS-coated beads also induces ICOS-L downmodulation from the cell surface in a few hours.[42,45]

We show here that ICOS-L levels in different cells and cell lines are drastically reduced within a few minutes of interaction with ICOS-expressing T cells. Previous data suggested that ICOS-induced downmodulation of cell surface ICOS-L is the consequence of proteinase-mediated "shedding" with the indirect or direct participation of ADAM10 and ADAM17.[40,45,46] However, although ADAM10 mediates ICOS-induced ICOS-L shedding from B cells, a significant effect of ADAM10 inhibitors on ICOS-L levels "in vitro" takes several hours, typically 20 to 24 hours.[40,45,46] Rather, our results using inhibitors indicate that proteinase mediated shedding does not have a major role in the fast ICOS-mediated downmodulation of cell surface ICOS-L that occurs within the first minutes of interaction. In contrast, we have found other mechanisms for fast ICOS-mediated removal of cell surface ICOS-L mediated in part by protein kinase C- (PKC), dynamin- and lipid raft-dependent endocytosis that is largely independent on chlatrin or caveolin, and also by ICOS-induced trans-endocytosis or trogocytosis.

2 | MATERIALS AND METHODS

2.1 | Mice

C57BL/6J mice (WT) and ICOS-deficient mice (ICOS-KO, B6.129S1-*Icos*^{tm1Flv}) aged eight to sixteen weeks were used. The mice were bred and housed at the animal care facilities of the Centro de Investigaciones Biológicas (CSIC, Madrid, Spain), under specific pathogen free conditions. The experimental procedures were approved by the Ethics

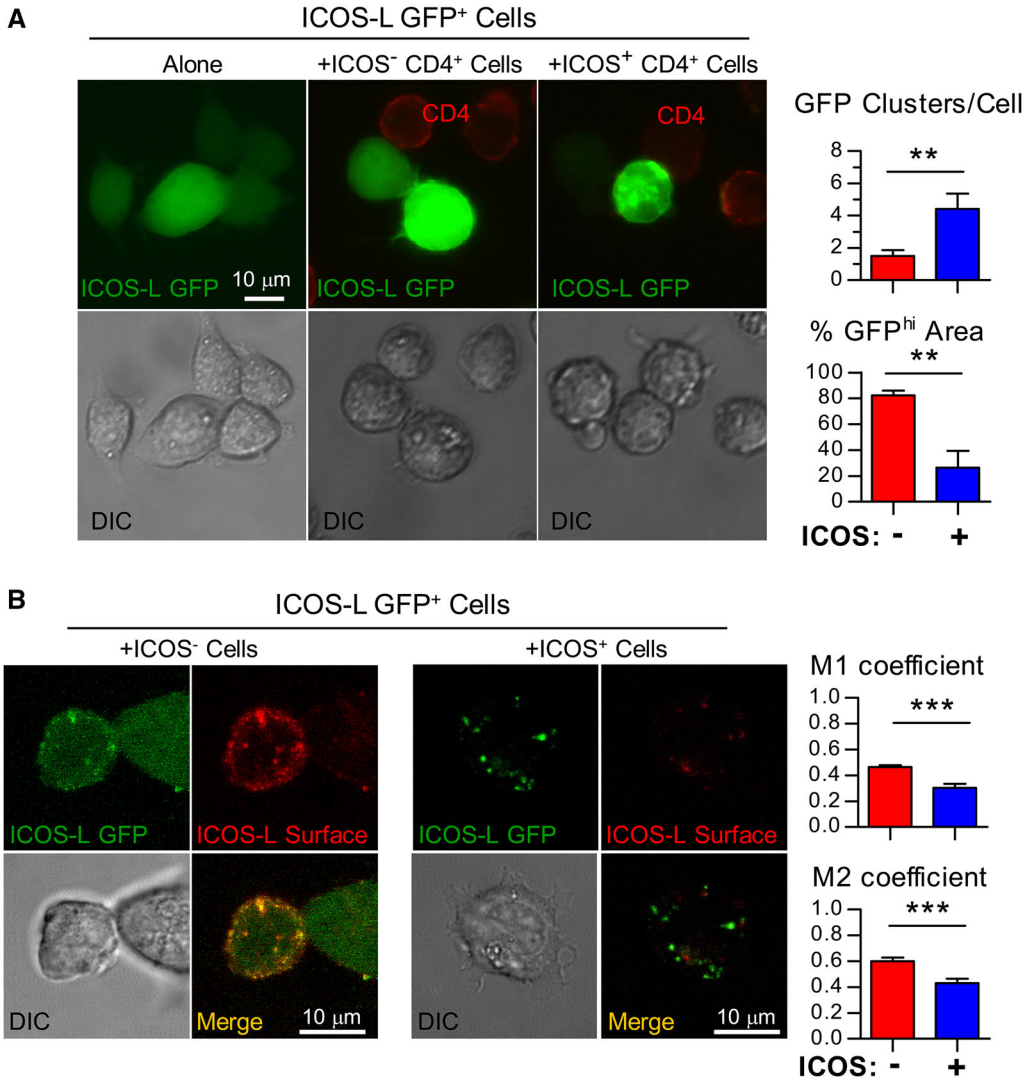

FIGURE 1 **Modulation of ICOS-L from the cell surface involves internalization. (A).** Cells of the B cell lymphoma M12.C3 expressing an ICOS-L GFP fusion protein (ICOS-L GFP$^+$) were incubated for 20 min at 37°C alone (left), or co-incubated with ICOS-expressing CD4$^+$ D10 T cells (+ICOS$^+$ CD4$^+$, right), or with an ICOS$^-$ mutant of D10 (+ICOS$^-$ CD4$^+$, center). Then, they were stained for surface CD4 to identify the T cells, and analyzed by multidimensional microscopy for ICOS-L GFP (green) or CD4 (red). Clumping of ICOS-L GFP in the presence of ICOS$^-$ cells (red bars) or ICOS$^+$ cells (blue bars) was quantified as the number of GFP fluorescence clusters/cell (GFP clusters/Cell, top graph) or the % of cell area with green fluorescence above threshold (% GFP^{hi} area, bottom graph). **(B).** M12 ICOS-L GFP$^+$ cells were co-incubated with ICOS$^-$ (left) or ICOS$^+$ (right) D10 cells, and surface ICOS-L stained (red). The cells were analyzed by confocal microscopy for distribution of ICOS-L GFP (green) and surface ICOS-L (red); colocalization was quantified as Manders (M1, M2) coefficients in the presence of cells lacking ICOS (ICOS$^-$, red bars) or cells expressing ICOS (ICOS$^+$, blue bars). Differences were analyzed by the Student's t test (**: $p < 0.01$; ***: $p < 0.001$)

and Animal Welfare Committees of CSIC and conducted according to local, national and European Union guidelines under project license PROEX 181/15 (to J.M.R.) approved by the Consejería de Medio Ambiente y Ordenación del Territorio, C.A. Madrid.

2.2 | Spleen T and B cells

CD4$^+$ spleen T cells from WT or ICOS-KO mice were activated with 2.5 μg/mL Concanavalin A for 72h; then isolated CD4$^+$ T cell blasts were expanded for further 48h with IL-2 as described in.[47] To obtain B cell blasts, spleen cells from ICOS-KO mice at 10^6 cells/mL in culture medium were activated for 72h with 30 μg/mL LPS. The cells were thoroughly washed before use in internalization assays.

2.3 | Cell lines

The cell lines used were the MHC Class II negative (I-A$^-$) M12.C3 mouse B cell lymphoma,[48] the mouse melanoma B16.F10, and the CHO chinese hamster ovary tumor cell. They were grown in Click's medium supplemented with 10% heat-inactivated fetal bovine serum and 50 μg/ml gentamicin (culture medium). The CD4$^+$ICOS$^+$ Th2 helper T cell line SR.D10 and its ICOS$^-$ mutant H4$^-$.A5 were

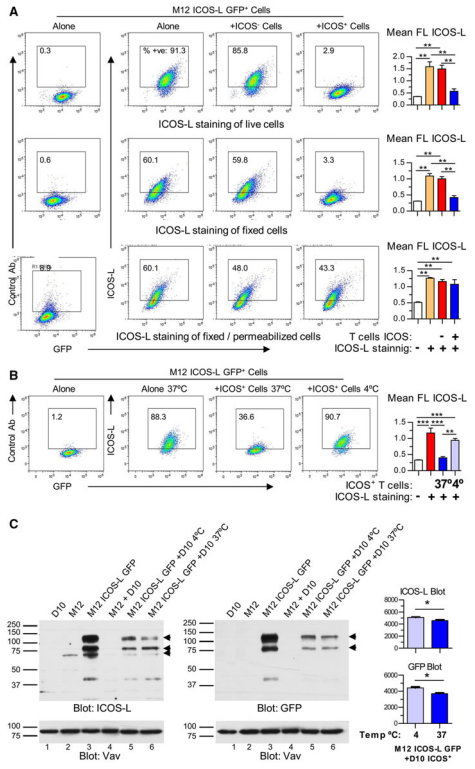

FIGURE 2 **Modulation of ICOS-L from the cell surface involves temperature-dependent internalization. (A).** M12 ICOS-L GFP$^+$ cells were incubated for 15 min at 37°C alone, or co-incubated with an ICOS$^-$ mutant of D10 CD4$^+$ T cells, or ICOS$^+$ D10 cells, then stained for ICOS-L and CD4, and analyzed by flow cytometry. M12 ICOS-L GFP$^+$ cells, gated as GFP$^+$ CD4$^-$ cells, were analyzed for ICOS-L staining before (top panel) or after cell fixation (center), or after fixation and permeabilization (lower panel). Graphs on the right show ICOS-L fluorescence (FL) of M12 ICOS-L GFP$^+$ cells incubated alone (orange bars), or with ICOS$^-$ T cells (red bars), or ICOS$^+$ T cells (blue bars). White bars indicate FL in cells stained with control antibody. Asterisks indicate significant differences between conditions as determined by one-way ANOVA. **(B).** ICOS-L modulation depends on temperature, as shown by M12 ICOS-L GFP$^+$ cells incubated for 20 min at 37°C alone, or co-incubated with ICOS$^+$ D10 cells at 37°C or at 4°C, as indicated. Cells were stained for ICOS-L and CD4, then M12 ICOS-L GFP$^+$ (GFP$^+$ CD4$^-$ cells) were gated and analyzed for ICOS-L staining. Numbers inside the histograms indicate the percentage of positive cells. The graph on the right shows FL in M12 ICOS-L GFP$^+$ cells incubated alone (red bar), or with ICOS$^+$ T cells at 37°C (blue bar) or 4°C (light blue bar). The white bar indicates FL in cells stained with control antibody. Asterisks indicate significant differences between conditions as determined by one-way ANOVA. **C.** Analysis by immunoblot of cell lysates from 0.5×10^6 M12 ICOS-L GFP$^+$ cells after incubation with 0.5×10^6 ICOS$^+$ D10 cells for 20 min at 4°C or 37°C, as indicated. Lysates of 10^6 cells each of D10 cells, or untransfected M12.C3 cells, or M12 ICOS-L GFP$^+$ cells, were included as controls. Blots were probed with ICOS-L- and GFP-specific antibodies; blots probed with anti-Vav antibodies were used as loading controls. Graphs (right) compare the corrected O.D. values (Arbitrary Units) of bands of 80 and 125 kDa in lanes 5 (4°C, light blue) and 6 (37°C, blue) of the ICOS-L blot (top graph) and the GFP blot (bottom graph). *: $p < 0.05$; **: $p < 0.01$; ***: $p < 0.001$. n.s.: not significant differences between triplicate determinations from one representative experiment of three **(A, B)** or two experiments **(C).** performed with similar results

grown in culture medium supplemented with IL-2, IL-4, and IL-1α, as described.[16,49,50]

2.4 | Antibodies and other reagents

Antibodies used were anti-CD4 RM4-5-APC (eBioscience) and RM4-5-AlexaFluor647 (BD Pharmingen), anti-CD19-FITC (ImmunoTools) and anti-CD19-PE (eBioscience); anti-B7h (Anti-CD275 HK5.3 and HK5.3-PE, eBioscience); Rabbit polyclonal antibodies anti-ERK (C-14), anti-Akt1/2 (H-136), and polyclonal goat anti-B7h (M-19) were from Santa Cruz Biotechnology. Anti-GFP (Abcam, 6673), HRP-rabbit anti-goat Ig (Dako, P0449) HRP-goat anti-rabbit Ig (Sigma, A-0545), goat anti-rat IgG Alexa568 and Alexa648 conjugates (Molecular Probes, A11077, A21247) were also used. FITC Cholera Toxin B (CTB) was from Sigma (C1655); Biotin-Cholera Toxin B and Alexa568-streptavidin conjugates were from Life Technologies (C34779 and S11226). Rabbit monoclonal anti-phospho-Akt(Ser473) (D9E) antibody was from Cell Signaling Technology.

Recombinant Mouse ICOS Fc Chimera was from R&D Systems (ref. 168-CS). Bafilomycin A, Blebbistatin, Brefeldin A, Chloroquine, Chlorpromazine, Colchicine, Cycloheximide, Cystamine, Cytocalasin B, Cytocalasin D, Dynasore, Genistein, LY294002, Methyl-β-Cyclodextrin, ML-7, PP-2, Phorbol Myristic acetate (PMA), and SB 203580 were from Sigma. Bisindolylmaleimide I (Gö6850), Ionomycin, ROCK inhibitor H-1152, Ro-31-8220 (Bisindolylmaleimide IX), U0126, and W-7 were from Calbiochem. The PI3-kinase inhibitors A-66 and IC-87114, and FAK inhibitors PF-573228 and PF-562271 were from Selleckchem. The proteinase inhibitors used were the α-secretase inhibitor GM 6001, β-Secretase Inhibitor IV, Dipeptidyl peptidase IV Inhibitor from Calbiochem; Z-VAD-FMK, pAB GP DL DA, 1,10-Phenantroline, and Phosphoramidon were from Sigma. The specificity of these reagents are summarized in Tables 1 and S1.

2.5 | Plasmids and mutagenesis

As expression vector for ICOS-L, the p-CMV6-Kan/Neo plasmid containing the cDNA for mouse B7h was used (pB7h plasmid, Origene TrueClone MC202216). Alternatively, the ICOS-L cDNA was amplified by PCR using primers and template cDNA prepared from mouse spleen. The primers used were:

5′-GCAAAGCTTGCTCGCACC**ATG**CAGCTAAAG-3′ (forward)
5′-GCAGGATCCGCGTGGTCTGTAAGTTCAAGC-3′ (reverse)

where Hind III and Bam HI sites are underlined, and the initial Met codon is indicated in bold. The amplified fragment was subcloned in-frame between the Hind III and Bam H1 sites of the pEGFP-N1 plasmid (Clontech) to generate plasmid pB7hGFP.

All pB7h and pB7hGFP mutants were generated with the QuikChange Lightning Site-Directed Mutagenesis Kit (Agilent). Mutants in conserved cytoplasmic residues (ICOS-L Arg_{300}-Ala, ICOS-L Ser_{307}-Ala, and ICOS-L Tyr_{308}-Phe) were obtained using the

TABLE 1 ICOS-induced ICOS-L downmodulation: Effect of inhibitors of endocytosis, cell cytoskeleton, protein kinase C, lysosomal function, autophagy, Src, MAPK, FAK, and PI3 kinases, or Calcium chelators

Endocytosis	Inhibitor	Inhibits ICOS-L Downmodulation[a,b]
Clathrin-Mediated Endocytosis	Chlorpromazine (50 μM)	+/-
Caveolin-Mediated Endocytosis	Genistein (100 μg/mL)	+
Dynamin GTPases/Endocytosis	Dynasore (100 μM)	++
Cholesterol Depletion/Lipid Raft-Dependent Endocytosis	Methyl-β-Cyclodextrin (10 mM)	++
Cytoskeleton	**Inhibitor**	**Inhibits ICOS-L Downmodulation[a,b]**
Actin polymerization	Cytochalasin D (10 μM)	++
Myosin ATPase	Blebbistatin (30 μM)	–
Myosin Light Chain Kinase	ML-7 (10 μM)	–
Tubulin (microtubule growth)	Colchicine (20 μM)	–
ROCK (Rho-dependent kinase)	H-1152 (5 μM)	–
Protein Kinase C	**Inhibitor**	**Inhibits ICOS-L Downmodulation[a]**
Protein Kinase C $\alpha, \beta, \gamma, \delta, \varepsilon$	Gö6850 (Bisindolylmaleimide I) (1-10 μM)	++[b]
Protein Kinase C $\alpha, \beta, \gamma, \delta, \varepsilon$	Ro-31-8220 (Bisindolylmaleimide IX) (5 μM)	++ [c]
Metabolic and Divalent ion blockers	**Inhibitor**	**Inhibits ICOS-L Downmodulation[a,b]**
Low Temp (4°C)	-	++++
Respiratory Chain	NaN_3 (15 mM)	–
Ca^{++}, Mg^{++} Chelation	EDTA (10 mM)	–
Ca^{++} Chelation	EGTA (10 μM)	–
Lysosomal function, Autophagy, Calcium	**Inhibitor**	**Inhibits ICOS-L Downmodulation[a]**
Lysosomal proton pump/Autophagosome-lysosome fusion	Bafilomycin A (0.5 μM)	–
Lysosomal/Autophagy inhibitor	Chloroquine (100 μM)	–
Golgi Transport	Brefeldin A (40 μM)	–
Transglutaminase 2	Cystamine (500 μM)	–
Calmodulin	W-7 (25 μM)	–
Src, MAPK, FAK, and PI3 kinases	**Inhibitor**	**Inhibits ICOS-L Downmodulation[a]**
Src Tyr Kinases Fyn, Hck, Lck	PP2 (5 μM)	–[c]
MEK-1 MAPK	U0126 (2.5 μM)	– [b]
P38 MAPK	SB203580 (1 μM)	–[b]

(Continued on next page)

TABLE 1 (Continued)

Src, MAPK, FAK, and PI3 kinases	Inhibitor	Inhibits ICOS-L Downmodulation[a]
Focal Adhesion Kinase (FAK)	FAK Inhibitor I (10 μM)	–[c]
Focal Adhesion Kinase (FAK)	FAK Inhibitor II (10 μM)	–[c]
PI3-K p110α	A66 (1 μM)	–[c]
PI3-K p110δ	IC87114 (1 μM)	–[c]
PI3-K p110$\alpha+\delta$	ETP-46321 (1 μM)	–[c]
PI3-K (All)	LY294002 (10 μM)	–[c]

M12 ICOS-L GFP cells were incubated with ICOS$^+$ D10 cells. ICOS-L staining in control assays of M12 ICOS-L GFP cells incubated with medium or with H4$^-$.A5 ICOS$^-$ D10 mutant cells was taken as a reference.
[a] Surface ICOS-L staining enhanced by 0–10% (–), 10–25% (+), 25–50% (++), 50–75% (+++), or > 75% (++++) of ICOS-L levels in M12 ICOS-L GFP cells incubated with medium or with H4$^-$.A5 ICOS$^-$ D10 mutant cells.
[b] Incubation 15 min.
[c] Incubation 60 min, fixed ICOS$^+$ cells.

following oligonucleotides (letters in bold indicate the changes in nucleotide sequence):

B7h Arg$_{300}$-Ala:

ICOS-L R300_A 1
*(5′-TCATCATATAC**GC**ACGCACGCGTCC-3′)*

ICOS-L R300_A 2
*(5′-GGACGCGTGCGT**GC**GTATATGATGA-3′)*

B7h Ser$_{307}$-Ala:

ICOS-L S307_A 1
*(5′-GTCCCCACCGA**GC**CTATACAGGACC-3′)*

ICOS-L S307_A 2
*(5′-GGTCCTGTATAG**GC**TCGGTGGGGAC-3′)*

B7h Tyr$_{308}$-Phe:

ICOS-L T_F 1
*(5′-GTCTTGGGTCCTGTA**A**AGCTTCGGTGGGGAC-3′)*

ICOS-L T_F 2
*(5′-GTCCCCACCGAAGCT**T**TACAGGACCCAAGAC-3′)*

Truncated forms of ICOS-L lacking part or all the cytoplasmic domain were obtained by mutation of Gly$_{310}$ (pB7h ΔG$_{310}$) or Arg$_{300}$ (pB7h ΔR$_{300}$) using the oligonucleotides:

B7h ΔGly$_{310}$:

ICOSL G310_TGA F
5′-CCCCACCGAAGCTATACATGACCCAAGACTGTAC-3′

ICOSL G310_TGA R 5′-GTACAGTCTTGGGTCATGTATAGCTTCGGTGGGG-3′

B7h ΔArg$_{300}$:

ICOSL R300_TGA F
5′-CGTTTCCTTCATCATATACTGACGCACGCGTCC-3′

ICOSL R300_TGA R
5′-GGACGCGTGCG TCA GTATATGATGAAGGAAACG-3′

To generate ICOS-L GFP fusion proteins lacking the intracytoplasmic sequence of ICOS-L, PCR were performed using pB7hGFP, one sense oligonucleotide (pEGFP-N1 MCS F) containing the Xho I and Hind III cloning sites of pEGFP-N1 and antisense oligonucleotides B7h BamH I Gly310 R and B7h BamH I Arg300 R that introduced new BamH I at residues Gly$_{310}$ and Arg$_{300}$:

pEGFP-N1 MCS F:
5′ CTCAGATCTCGAGCTCAAGCT 3′

B7h BamHI Arg300 R:
5′ GGTGGATCCCTGTATATGATGAAGGAAACGAATGC 3′

The PCR products were subcloned between sites Xho I and BamH I of pEGFP-N1 to obtain pB7hΔR$_{300}$GFP. Mutant plasmids were selected according to the manufacturer's instructions, and their sequence confirmed.

To obtain ICOSmCherry fusion proteins, ICOS cDNA was obtained by RT-PCR using SR.D10 RNA as template and the oligonucleotides ICOS HindIII F (sense) and ICOS EcoRI R (antisense), that included new HindIII and EcoRI restriction sites (underlined) flanking the mouse ICOS coding sequence (Met$_1$ to Ser$_{200}$):

ICOS HindIII F:
GAGCTCAAGCTTATGAAGCCGTACTTCTGCCG

ICOS EcoRI R:
CTGCAGAATTCCTGAGGTCACACCTGCAAGT

The PCR products were subcloned in the pcDNA3.1/V5-His-TOPO plasmid (Invitrogen) and the sequence of the insert was confirmed. Then, the HindIII-EcoRI fragment containing the ICOS sequence was subcloned between the HindIII and EcoRI sites of the pEF1α-mCherry-N1 vector (Takara Clontech) to obtain the plasmid pICOSmCherry.

2.6 | Transfection

Transfectants of different cell lines were generated by nucleofection of 1.5-2 $\times$ 10^6 cells plus 2 μg of plasmid DNA in 100 μL of nucleofection solution V (Lonza) and programs L-13 (M12.C3), P-20 (B16.F10), U-24 (CHO), and X-01 ($H4^-$.A5) of the Nucleofector I device (Lonza), according to the manufacturers' instructions. After 24 h, the culture medium was changed and Geneticin added. Cells were used within 48–72 h after transfection, or further expanded and selected for expression of ICOS-L, ICOS-L GFP, mCherry, or ICOSmCherry by flow cytometry and cloning of stable transfectant cells.

2.7 | ICOS-L modulation assay

In a standard assay, ICOS-L GFP^+ cells of the M12.C3 lymphoma transfected with pB7hGFP (M12 ICOS-L GFP^+ cells) and SR.D10 $ICOS^+$ cells were washed and adjusted to 10^7 cells/ml in culture medium. Then, 50 μL (0,5 $\times$ 10^6) of each cell suspension were mixed in round-bottom 96 well plates and cultured for 15 min or the time indicated at 37°C in a CO_2 incubator. All other procedures were strictly performed in the cold. After washing with PBS/0.1% BSA/0.1% NaN_3 (staining buffer), the cells were stained with anti-B7h-PE and anti-CD4-APC. Control assays included M12 ICOS-L GFP^+ cells mixed with $ICOS^-$ mutant cells or with culture medium as well as staining with isotype IgG controls. The stained cells were washed and fixed with 1% paraformaldehyde in PBS before flow cytometry acquisition in a Beckman Coulter FC-500 flow cytometer and analysis by FlowLogic software, or in a BD LSRFortessa™ cytometer and the BD FACSDiva™ software, or the FlowJo software (Tree Star, Ashland, OR). For assays in the presence of inhibitors, ICOS-L-expressing cells were pre-incubated for 30 min with the inhibitor, and distributed in wells. $ICOS^+$ cells were then added, and the plates centrifuged in the cold. After removing the supernatants, the cells were resuspended in 0.1 ml of culture medium containing the corresponding inhibitor. As controls, cells were incubated with medium containing the same volume of dimethyl sulfoxide (DMSO), or the solvent used.

The same approach was used to assay ICOS-induced ICOS-L modulation in ICOS-L GFP^+ (pB7hGFP) transfectants of the B16.F10 melanoma or the CHO chinese hamster ovary cell lines, or ICOSmCherry transfectants of the $ICOS^-$ SR.D10 mutant $H4^-$.A5, or B and T cell blasts. Since the ICOS-L is sensitive to trypsin, when adherent cells were used they were detached from culture plates by incubation for 15 min at 37°C in 2 mM EDTA/PBS and pipetting. Where indicated, SR.D10 $ICOS^+$ cells were previously fixed with 4% paraformaldehyde (5 min at 37°C) and washed with cold staining buffer. To stain both surface and intracellular ICOS-L, the cells were fixed with 4% paraformaldehyde, permeabilized with saponin and stained in the presence of saponin as described in.[51] Where needed, cell sorting was performed using a BD FACS Aria I™ flow cytometer (BD Biosciences).

2.8 | Cell lysis and Immunoblot

Cells were washed with PBS and lysed (1.5-2 $\times$ 10^7 cells/ml) in lysis buffer (Tris/HCl 50 mM, pH 7,6, NaCl 150 mM, 1% Tritón X-100, Cl_2Mg 1 mM, EGTA 1 mM, Na_3VO_4 1 mM, plus a protease inhibitor cocktail (Selleckchem K4000)). After 15 min on ice, the lysates were centrifuged (600 xg, 5 min) and the supernatants mixed v:v with 2xSDS PAGE sample buffer. The proteins were separated in 10% PAGE gels and immunoblot performed as described.[16]

2.9 | Microscopy

Cells (0.3-1 $\times$ 10^5) were seeded on microscopy chamber wells (1 μ-Slide 8 well, Ibidi) coated overnight with poly-L-Lysine (1 mg/ml, 4°C) and washed. The attached cells were fixed with 4% paraformaldehyde in PBS (2 min at 37°C), washed with staining buffer, and mounted with ProLong Diamond antifade mountant (Molecular Probes).

Where needed, intracellular staining was performed after permeabilization in seeded, fixed cells as described above.

Multidimensional microscopy was performed on a Leica AF6000 LX system microscope (Mannheim, Germany); images were captured using a 40.0 $\times$ 0.75 DRY objective lens with the Hg-arc lamp.

Confocal microscopy analysis was performed in a Leica TCS-SP2-AOBS-UV ultraspectral confocal microscope. Immunofluorescence analysis was done using a 63 $\times$ 1.4 objective lens at 0.5 μm intervals. Signals from different fluorescent probes were taken in parallel. Image processing was performed using the ImageJ 1.54p NIH public software and Adobe Photoshop (Adobe Systems, Mountain View, CA). Manders thresholded colocalization coefficients (M1, M2) were calculated using the ImageJ 1.54p NIH software.

2.10 | Separation of detergent-insoluble membrane microdomains

Detergent-insoluble microdomains enriched in glycosphingolipids and cholesterol (DIM), were separated as described,[52,53] with minor modifications. Cells (0.5-1 $\times$ 10^8) were lysed in 1 ml of 0.5% Triton X-100 in MBS buffer (25 mM MES, 150 mM NaCl, pH 6.5 1 mM EDTA Na_3VO_4 1 mM, and protease inhibitor cocktail, pH 6.5). The lysate was homogeneized with 10 strokes of a loose-fitting Dounce homogenizer, and centrifuged 10 min at 900 xg. The supernatant was mixed v:v with 85% sucrose in MBS, set on a 12 ml ultracentrifuge tube and overloaded with 5 ml of 35% sucrose in MBS and 5 ml of 5% sucrose in MBS. The samples were centrifuged 16–18 h at 200.000 xg at 4°C. Fractions of 1 ml were taken and analyzed for GM-1 content as an indicator of DIM. Proteins in the different fractions were separated by SDS-PAGE and analysed by immunoblot.

2.11 | Statistics

Data were analyzed using the GraphPad Prism 5 software (GraphPad Software, San Diego, CA, USA). Comparison of experimental groups was performed with one-way or two-way ANOVA, or unpaired, two-tailed Student´s t test. Results are expressed as the mean ± standard error of the mean (SEM). Statistical significance was set at $p < 0.05$.

3 | RESULTS

3.1 | ICOS / ICOS-L interaction induces fast surface internalization of ICOS-L

Previous data have shown that interaction with ICOS reduces ICOS-L levels in the cell surface.[45] Part of the ICOS-L can be detected by ELISA in the supernatant after three hours, in a proteinase-dependent process that can be inhibited with the α-Secretase inhibitor GM 6001.[45] In agreement with these data, we observed that ICOS-L levels in the surface of lymphoma cells expressing an ICOS-L GFP fusion protein (M12 ICOS-L GFP$^+$) were markedly reduced upon co-culture with ICOS$^+$ cells for less than 60 min (i.e., 20 min). This phenomenon was ICOS-dependent, as no modulation was observed when ICOS$^-$ D10 cell mutants were used. Surprisingly, our attempts to inhibit ICOS-L modulation with the α-Secretase inhibitor GM 6001, or other proteinase inhibitors failed to significantly reduce fast ICOS-L disappearance (Table S1). Similar downmodulation was observed in cells expressing normal, wild-type ICOS-L instead of ICOS-L GFP, as well as in assays determining ICOS-L expression in B cells after interaction with T cell blasts from wild type or ICOS-deficient mice (Supplementary Figure S1). These results suggested that proteinase-mediated removal of ICOS-L was not the main mechanism involved in this phenomenon, and that fast downmodulation can be induced using activated primary spleen cells.

We then searched for alternative mechanisms of surface ICOS-L modulation, including internalization. Fluorescence microscopy analysis of GFP distribution in M12 ICOS-L GFP$^+$ cells before or after incubation for 20 min with ICOS$^+$ D10 cells indicated a clear change in GFP distribution to form intracellular clumps, whereas GFP distribution was uniform upon incubation of the cells alone or in the presence of cells that do not express ICOS (fig. 1A). Further evidence for internalization came from confocal microscopy studies showing that, in the absence of ICOS stimulus, there was abundant surface ICOS-L which co-localized with GFP. In contrast, the contact with ICOS-expressing cells induced the appearance of GFP patches inside the cells with no or low surface ICOS-L staining (fig. 1B). Modulation of ICOS-L run in parallel with ICOS-dependent intracellular signaling, as shown by strong phosphorylation of Akt (Supplementary Figure S2).

In agreement with the above data, Figure 2 shows that the level of ICOS-L staining after 20 min incubation of M12 ICOS-L GFP$^+$ cells with ICOS$^+$ D10 cells was largely recovered after cell permeabilization, confirming the intracellular location of most ICOS-L under these conditions (fig. 2A).

Interestingly, co-incubation of M12 ICOS-L GFP$^+$ cells and ICOS$^+$ D10 cells in the cold largely prevented modulation of surface ICOS-L (fig. 2B). Yet, in the lysates of cells incubated at 37°C there was just a modest decrease in the amount of ICOS-L as compared to cells incubated at 4°C, as detected by immunoblot (compare lanes 5 and 6, Figure 2C, left). Immunoblot with GFP-specific antibodies yielded similar results (lanes 5 and 6, Figure 2C, right). This is unlike one would expect in the event of ICOS-L shedding, where the amount of ICOS-L in lysates from cells at 37°C should be comparatively much lower than the amount of remaining intracellular GFP. As shown in the figure, monomers as well as oligomers of ICOS-L were detected, in agreement with previous data.[54] Taken together, these data show that internalization, rather than shedding, is the main mechanism for the early removal of surface ICOS-L induced by ICOS in this system.

3.2 | ICOS-L modulation by live or fixed ICOS$^+$ cells

As shown in Figure 3, ICOS-L modulation from the surface of the M12 B cell lymphoma is a very fast process. According to the time course, less than 50% of the initial ICOS-L remained available to antibody in the cell surface after 15 min of incubation with ICOS$^+$ cells, and remains low for up to 120 min (fig. 3A). Interestingly, although some level of ICOS-L modulation was observed when fixed ICOS$^+$ cells were used, the process was partial, slow and impaired when compared to modulation induced by live ICOS$^+$ cells at the times considered (fig. 3B). To analyze whether the internalized ICOS-L underwent proteolysis, we determined by immunoblot the molecular species present in cell lysates before or after co-incubation for 90 min with ICOS$^+$ T cells. The data in Supplementary Figure S3 show no clear indication of proteolytic degradation upon internalization (Fig S3a, b). Then, we assessed whether removing ICOS$^+$ T cells by cell sorting after internalization would allow re-expression of ICOS-L in the cell surface. The data in Supplementary Figure S3c show that surface ICOS-L levels are readily restored after 2h culture, but this requires "de novo" protein synthesis, as surface ICOS-L remains low in the presence of Cycloheximide.

3.3 | Role of conserved cytoplasmic residues in ICOS-L modulation

To analyze the internalization mechanisms of ICOS-L, we searched for internalization motifs in the cytoplasmic sequence of mouse ICOS-L. Although some di-leucine motifs could be found in the cytoplasmic domain of ICOS-L of some mammalian species, neither these nor other known internalization motifs were present in the mouse ICOS-L sequence (See data in Table S2 for comparison of known mammalian ICOS-L sequences). Nevertheless, the participation of endocytic mechanisms in ICOS-L modulation was analyzed using two approaches, namely, the mutation of ICOS-L sequence, and the use of inhibitors.

Comparison of ICOS-L sequences from different species shows that a number of residues within the cytoplasmic domain are highly conserved (Table S2). Particularly, a juxtamembrane sequence motif (R-X-R-X(4-5)-SY) is frequently found in the sequences considered. In this

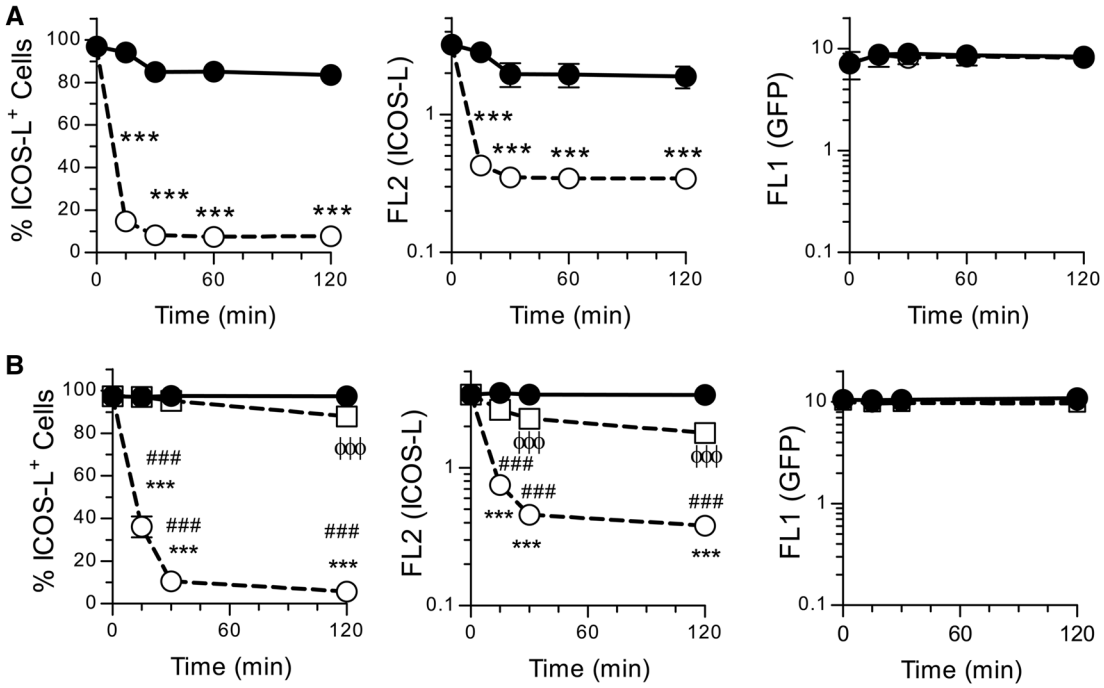

FIGURE 3 **ICOS-dependent modulation of cell surface ICOS-L is a fast process that is impaired by fixation of ICOS$^+$ cells. (A).** M12 ICOS-L GFP$^+$ cells were incubated at 37°C for different times alone (closed symbols) or with ICOS$^+$ D10 cells (open symbols), then stained in the cold for ICOS-L and CD4. M12 ICOS-L GFP$^+$ cells (GFP$^+$ CD4$^-$ cells), were gated and analyzed for ICOS-L and GFP fluorescence. Data shown as per cent ICOS-L$^+$ cells (left panel), or mean ICOS-L fluorescence (middle panel), or mean GFP fluorescence (right panel). Asterisks indicate significant differences between conditions as determined by two-way ANOVA (***: $p < 0.001$). **(B).** M12 ICOS-L GFP$^+$ cells were incubated at 37°C for different times alone (closed circles, solid line) or with ICOS$^+$ D10 live cells (open circles, dashed lines), or with fixed ICOS$^+$ D10 cells (squares, dashed line), then fluorescence analyzed and shown as in **A).** Symbols indicate significant differences ($p < 0.001$) in fluorescence of ICOS-L GFP$^+$ cells in the presence or absence of fixed ICOS$^+$ cells ($\phi\phi\phi$), or between ICOS-L GFP$^+$ cells plus or minus ICOS$^+$ live cells (***), or between ICOS-L GFP$^+$ cells plus live or fixed ICOS$^+$ cells (###), as determined by two-way ANOVA

regard, Hedl et al. have shown that at least the Arg residues located close to the membrane and the Ser residue play a functional role in ICOS-L signaling in human DC.[20] Mutants of mouse ICOS-L in residues Arg_{300}, Ser_{307} and Tyr_{308} were generated and expressed in M12.C3 lymphoma or B16 melanoma cells (see sequence in Figure 4A). As shown in Figure 4B-D, the modulation of ICOS-L induced by ICOS$^+$ cells was not impaired in these mutants. This suggests that, unlike the signaling of ICOS-L described by Hedl et al. in human DC,[20] changes in these conserved aminoacids are not critical to fast ICOS-induced ICOS-L internalization in the mouse.

3.4 | Effect of metabolic inhibitors on ICOS-L modulation

Since mutation of these conserved residues did not give a clue as to the mechanism(s) involved in ICOS-L internalization, further analysis of the mechanisms involved was performed using a number of reagents with potential effect on endocytosis. The results summarized in Table 1 show that ICOS-L downmodulation was partially dependent on the Dynamin GTPase and sensitive to depletion of membrane cholesterol, as shown by the effect of Dynasore and methyl-β-cyclodextrin, respectively (Table 1, Figure 5). Inhibitors of clathrin- (Chlorpormazine) or caveolin-mediated internalization (Genistein) had minor effects on ICOS-L downmodulation (Table 1). On the other hand, inhibitors of actin polymerization and protein kinase C significantly inhibited ICOS-induced internalization (Table 1, Figure 6), and low temperature blocked the phenomenon (Table 1, Figure 2). A number of other reagents that inhibit endocytosis or other related processes in other experimental systems, or are known to participate in ICOS-L signaling had no detectable effect, including inhibitors of lysosomal function, autophagy, Calmodulin, as well as inhibitors of Src and FAK tyrosine kinases, MAP kinases, and PI3 kinases (Table 1).

3.5 | ICOS-L is present in lipid rafts

The effect of cholesterol depletion on ICOS-L downmodulation suggested a role for cholesterol-rich, detergent-resistant lipid rafts. Since ICOS is largely absent from the lipid rafts,[55] the effect could be mediated by the ICOS-L. Indeed, separation of M12 ICOS-L GFP cell lysates by ultracentrifugation in discontinuous sucrose gradients and analysis of the fractions by immunoblot confirmed that part of the ICOS-L was present in the lipid raft-enriched (i.e. GM-1-enriched) fractions (fig. 7).

Interestingly, mouse ICOS-L residues 294 to 303 (VSFIIYRRTR), that includes part of the transmembrane domain, comprise a sequence

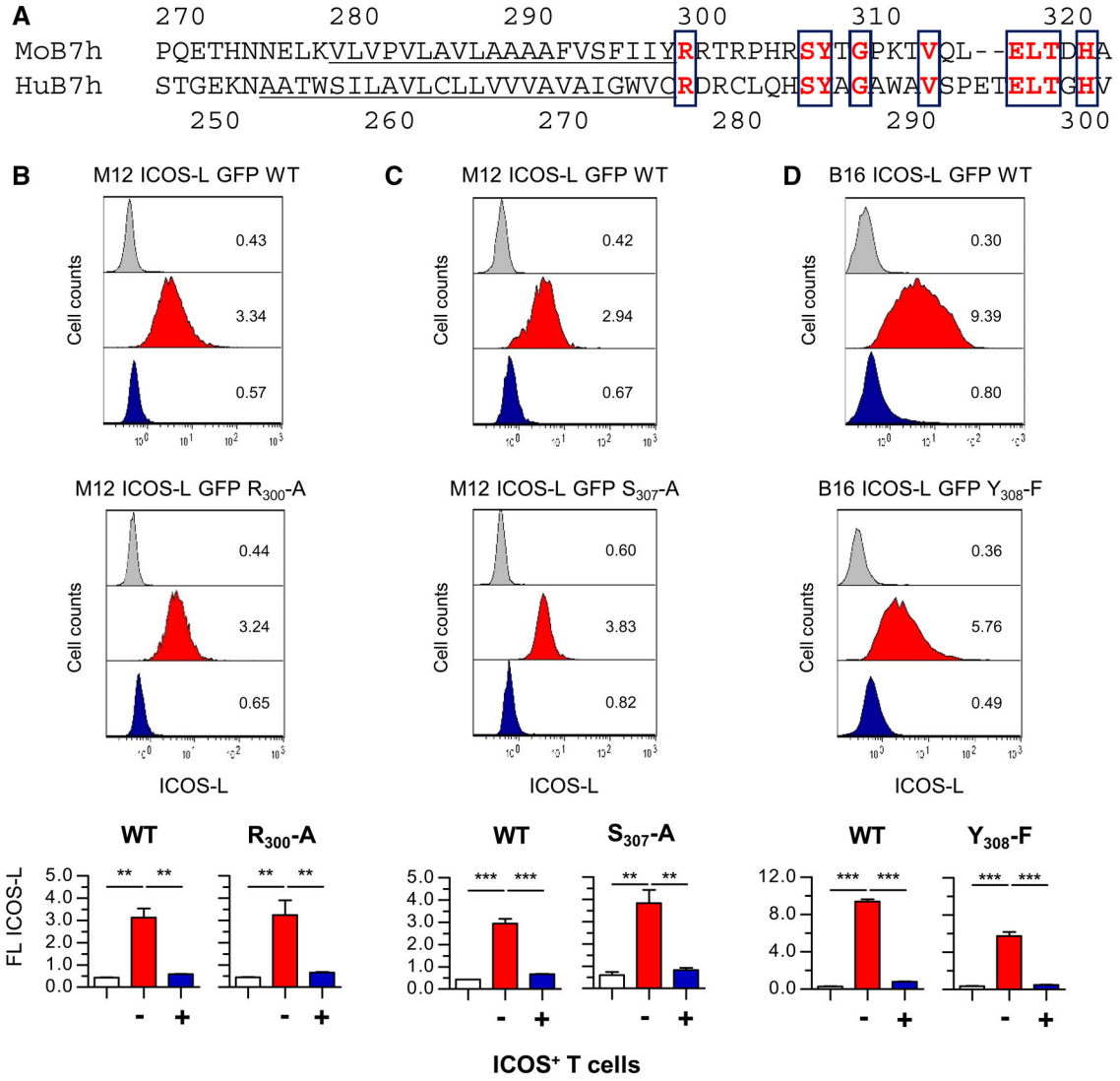

FIGURE 4 **Mutation of single conserved residues in the cytoplasmic domain of ICOS-L does not affect ICOS-induced downmodulation. (A).** Comparison of transmembrane (underlined) and cytoplasmic domains of mouse (Mo B7h, sequence: gi22137739) or human (Hu B7h, sequence: gi426393243) ICOS-L. Conserved residues in bold are boxed. **B.** M12.C3 cells transfected with wild type mouse ICOS-L (M12 ICOS-L GFP$^+$ WT cells, top) or with a mutated form of ICOS-L (Arg$_{300}$ to Ala, M12 ICOS-L GFP R_{300}-A, bottom) were incubated at 37°C for 30 min with ICOS$^-$ (red histogram) or ICOS$^+$ D10 cells (blue histogram), then stained in the cold for ICOS-L and CD4, and ICOS-L GFP$^+$ cells (GFP$^+$ CD4$^-$ cells) were gated and analyzed for surface ICOS-L. **C.** M12.C3 cells transfected with wild type mouse ICOS-L (M12 ICOS-L GFP$^+$ WT cells, top) or with a mutated ICOS-L (Ser$_{307}$ to Ala, M12 ICOS-L GFP S_{307}-A, bottom) were incubated with ICOS$^-$ (red histogram) or ICOS$^+$ D10 cells (blue histogram), and stained, gated, and analyzed for surface ICOS-L, as in **(B). D.** B16.F10 cells were transfected with wild type mouse ICOS-L (B16 ICOS-L GFP$^+$ WT cells, top) or with a mutated ICOS-L (Tyr$_{308}$ to Phe, B16 ICOS-L GFP Y_{308}-F, bottom) were incubated at 37°C for 30 min with ICOS$^-$ (red histogram) or ICOS$^+$ D10 cells (blue histogram), then stained in the cold, GFP$^+$ CD4$^-$ B16.F10 cells were gated, and analyzed for surface ICOS-L. Grey histograms are from cells stained with a control antibody. Numbers inside the histograms indicate the mean fluorescence from the graphs below. Graphs in the bottom show the mean ICOS-L fluorescence in cells transfected with WT or mutant ICOS-L. Asterisks (**: $p < 0.01$; ***: $p < 0.001$) indicate significant differences between samples as determined by one-way ANOVA of ICOS-L fluorescence between cells incubated with ICOS$^-$ cells (red bars) or with ICOS$^+$ cells (blue bars) from four (M12 ICOS-L GFP R_{300}-A; B16 ICOS-L GFP Y_{308}-F) or three (M12 ICOS-L GFP S_{307}-A) different clones. White bars represent data from cells stained with a control antibody

similar to Cholesterol Recognition/interaction Amino acid Consensus (CRAC) sequence motifs ([L/V]-X(1-5)-Y-X(1-5)-[R/K]) or CRAC-like sequence motifs ([L/V]-X(1-5)-F-X(1-5)-[R/K]) (EMBOSS: fuzzpro (http://emboss.bioinformatics.nl/cgi-bin/emboss/fuzzpro). Thus, interaction with cholesterol might facilitate the presence of ICOS-L in lipid rafts.

3.6 | Modulation of ICOS-L lacking the cytoplasmic tail

To further determine the basis for ICOS-induced ICOS-L downmodulation, mutants were obtained lacking the cytoplasmic domain of ICOS-L (ICOS-L GFP $R_{300}\Delta$). The ICOS-L $R_{300}\Delta$ mutant lost Ser and Arg residues that are important to huICOS-L function[20] and participate in

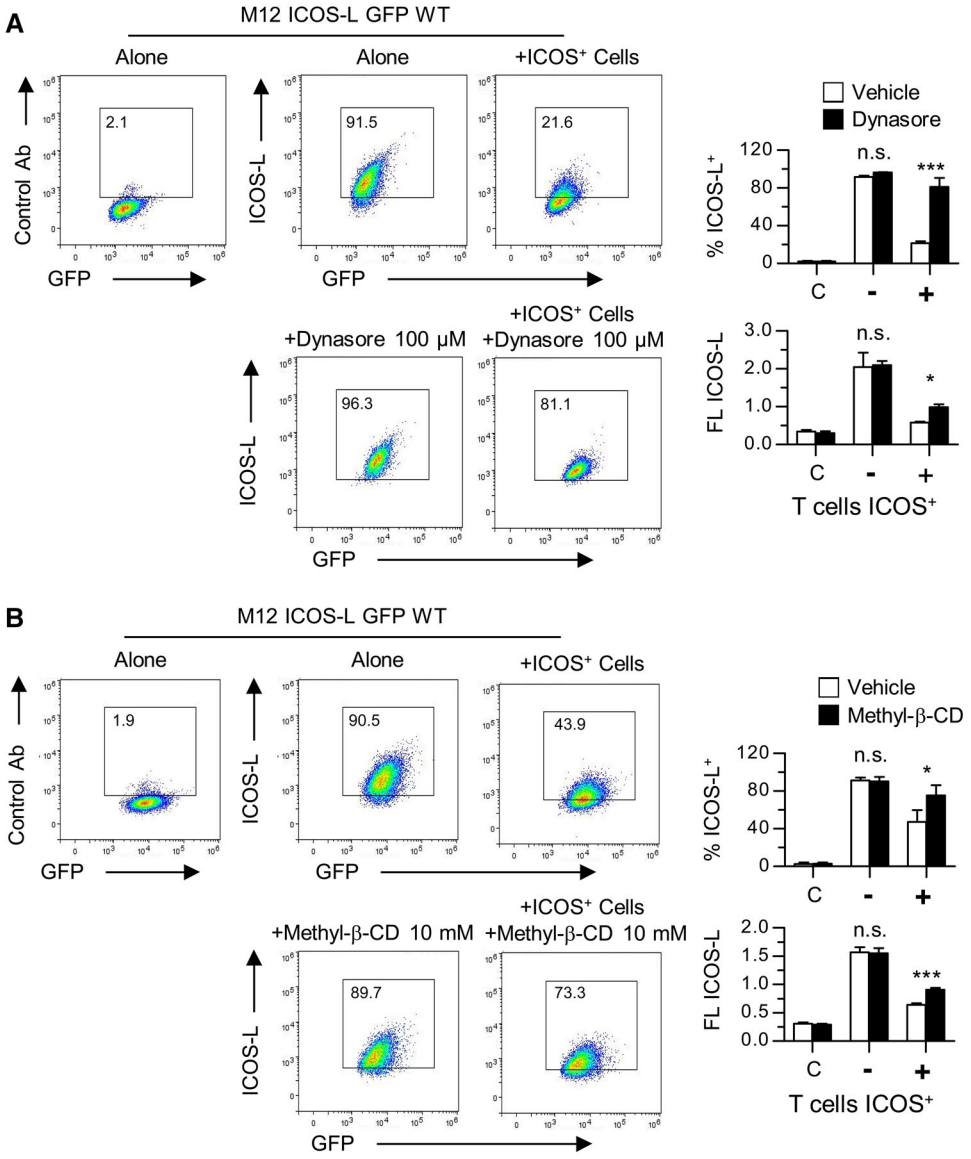

FIGURE 5 **Effect on ICOS-induced downmodulation of the ICOS ligand of**: **(A).** the Dynamin GTPase inhibitor Dynasore, or **(B).** membrane cholesterol depletion with Methyl-β-cyclodextrin. M12.C3 cells transfected with wild type mouse ICOS-L GFP (M12 ICOS-L GFP WT) were incubated at 37°C for 15 min with ICOS$^+$ D10 cells in the presence of Dynasore or Methyl-β-cyclodextrin, as indicated. Then, the cells were stained in the cold, M12 ICOS-L GFP cells were gated as GFP$^+$ CD4$^-$ cells, and analyzed for surface ICOS-L levels. Numbers inside the histograms indicate the percentage of ICOS-L positive cells. The graphs show the percentage of ICOS-L$^+$ cells, or the mean ICOS-L fluorescence, in M12 cells incubated alone (-) or with ICOS$^+$ D10 cells (+) in the absence (open bars) or the presence (black bars) of Dynasore or Methyl-β-cyclodextrin, as indicated. Bars in the left **(C).** are data from cells stained with a control antibody. Asterisks (*: $p < 0.05$; ***: $p < 0.001$) indicate significant differences between cells incubated with or without Dynasore or Methyl-β-cyclodextrin, as determined by two-way ANOVA. n.s.: not significant. Data from triplicate determinations of one representative experiment of two experiments performed with similar results

the CRAC motifs. These constructs were transfected into CHO cells, and the transfectants were analyzed for surface ICOS-L expression after interaction with ICOS$^+$ cells. As shown in figure 7, removal of the cytoplasmic domain barely inhibited ICOS-induced ICOS-L downmodulation (fig. 7b). This suggests that lipid rafts can help in ICOS-L endocytosis, but are not essential to the process. This, plus the results of point mutation, indicated that neither membrane-proximal cytoplasmic residues, nor the VSFIIYRRTR CRAC motif are essential to ICOS-L internalization.

3.7 | Transfer of ICOS into ICOS-L expressing cells during modulation

As an alternative or a complement to endocytosis, we examined trans-endocytosis (trogocytosis) as a possible mechanism for ICOS-induced ICOS-L internalization. This was shown, first, by the detection of ICOS in the surface of ICOS-L$^+$ cells after co-culture with ICOS$^+$ cells (fig. 8A, lower left, blue histogram). This phenomenon run in parallel with downmodulation not only of surface ICOS-L in ICOS-L$^+$ cells (fig. 8A, top left, blue histogram) but, more importantly, with downmodulation

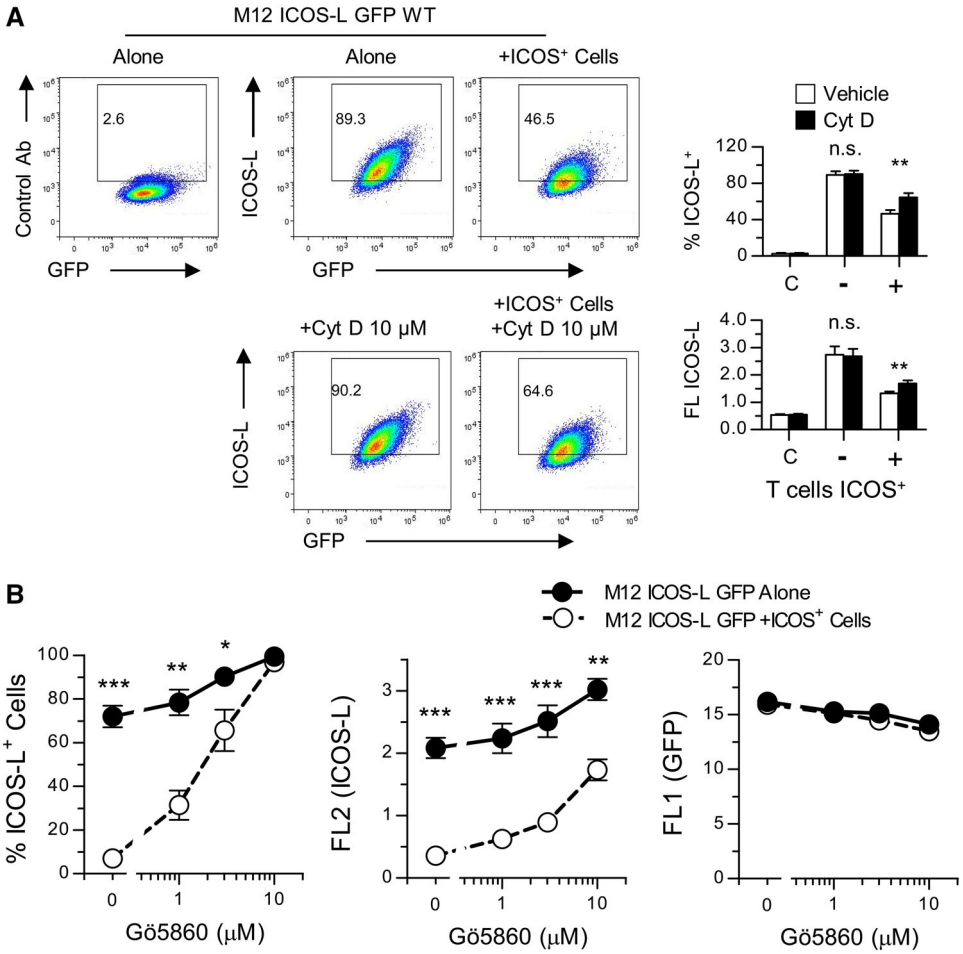

FIGURE 6 **Effect of the inhibitor of actin polymerization Cytochalasin D (A).** and the Protein Kinase C inhibitor Gö6850 **(B).** on the downmodulation of ICOS-L induced by ICOS$^+$ cells.

(A). M12 ICOS-L GFP cells were incubated at 37°C for 15 min alone or with ICOS$^+$ D10 cells in the presence or absence of Cytochalasin D. Cells were stained and M12 ICOS-L GFP cells, gated as GFP$^+$ CD4$^-$ cells, were analyzed for surface ICOS-L. Graphs show the percentage of ICOS-L$^+$ cells, or the mean ICOS-L fluorescence, in M12 cells incubated alone (-) or with ICOS$^+$ D10 cells (+) in the absence (open bars) or the presence (black bars) of Cytochalasin D, as indicated. Bars in the left **(C).** are data from cells stained with a control antibody. Asterisks (**: $p < 0.01$) indicate significant differences between cells incubated with or without inhibitor as determined by two-way ANOVA. n.s.: not significant. **B.** M12 ICOS-L GFP cells were incubated at 37°C for 15 min alone or with ICOS$^+$ D10 cells in the presence of different concentrations of the Protein Kinase C inhibitor Gö6850. Graphs represent the percentage of ICOS-L$^+$ cells (left), or the mean ICOS-L fluorescence (center), or GFP fluorescence (right) in M12 cells incubated without (closed symbols) or with ICOS$^+$ D10 cells (open symbols). Asterisks (*: $p < 0.05$; **: $p < 0.01$; **: $p < 0.001$) indicate significant differences between cells incubated with or without ICOS$^+$ D10 cells, as determined by two-way ANOVA. Data from triplicate determinations of one representative experiment of two experiments performed with similar results

of surface ICOS in the ICOS$^+$ T cells (fig. 8B, left, blue histogram). These phenomena could not be observed using control cells that did not express ICOS-L (fig. 8A, lower right, blue histogram), or ICOS (fig. 8A, red histograms), or in other surface markers of T cells (i.e. CD4) (fig. 8B, right, blue histogram).

To confirm the specific transfer of ICOS to ICOS-L expressing cells, we used ICOS-deficient H4$^-$.A5 cells transfected with plasmids coding for ICOSmCherry fusion proteins, or transfected with mCherry vector alone. Cells transfected with ICOSmCherry vectors expressed high levels of ICOS and mCherry, and possessed a characteristic feature of ICOS ligation, namely ICOS-induced changes in cells shape, particularly cell elongation (Supplementary Figure S4). When ICOSmCherry transfectants were co-incubated with cells expressing ICOS-L, transfer of mCherry fluorescence to the GFP$^+$ ICOS-L$^+$ CHO cells was observed (fig. 8C, left, blue histogram). In contrast, transfer of ICOSmCherry fluorescence to cells lacking ICOS-L was negligible (fig. 8C, left, red histogram), as was the transfer of red fluorescence from cells expressing mCherry alone (fig. 8C, right). Confocal analysis of individual GFP$^+$ ICOS-L$^+$ M12 lymphoma cells incubated with ICOSmCherry transfectants of the CD4$^+$ ICOS-deficient cell line H4$^-$.A5 confirmed ICOS-specific internalization of ICOS-L GFP and co-localization of ICOS-L GFP with ICOSmCherry at intracellular vesicles or juxtamembrane locations (fig. 8D, left). This was not observed using T cells transfected with mCherry alone (fig. 8D, right). All these data indicate that

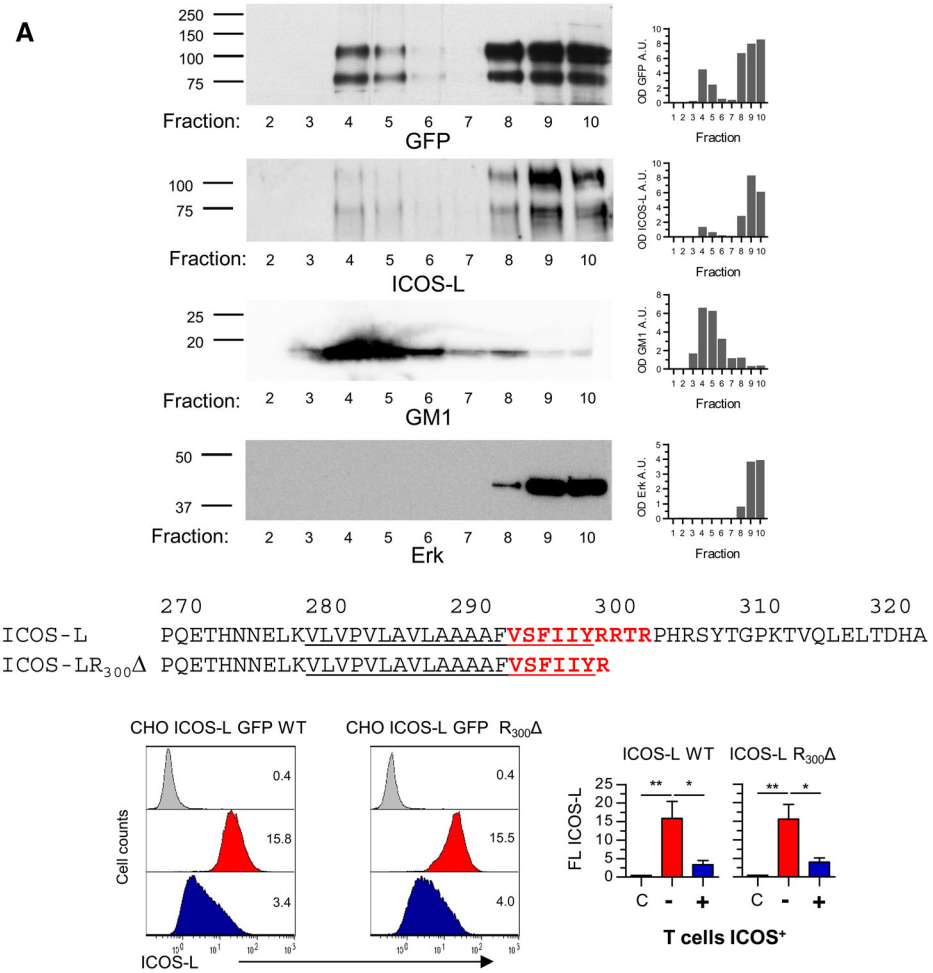

FIGURE 7 **ICOS-L is present in cholesterol-rich detergent-insoluble membrane lipid rafts, and role of the cytoplasmic domain and CRAC motifs in ICOS-L internalization.**

(A). M12 ICOS-L GFP cell lysates were ultracentrifuged in a sucrose gradient, and fractions from 2 (top) to 10 (bottom) were separated by SDS-PAGE. Then, the presence of ICOS-L in each fraction was detected by immunoblot using anti-ICOS-L- or GFP-specific antibodies (top panels). Membrane rafts were determined using Cholera toxin B subunits to detect the GM1 ganglioside, whereas fractions poor in lipid rafts were detected using anti-Erk antibodies, as indicated (bottom panels). Numbers in the left indicate approximate MW in kDa.

(B). Partial sequence of mouse ICOS-L (MoB7h). The CRAC (cholesterol recognition/interaction amino acid consensus) sequence VSFIIYRRTR in mouse ICOS-L is indicated in bold red letters, and includes part of the transmembrane domain (underlined). CHO cells transfected to express fusion proteins of GFP and wild type mouse ICOS-L (CHO ICOS-L GFP WT) or ICOS-L lacking the cytoplasmic domain (CHO ICOS-L GFP $R_{300}\Delta$) were incubated at 37°C for 15 min with ICOS-deficient $H4^{-}$.A5 cells (red histograms) or $ICOS^{+}$ D10 cells (blue histograms), then stained in the cold for ICOS-L and CD4. ICOS-L GFP cells (GFP^{+} $CD4^{-}$ cells) were gated and analyzed for surface ICOS-L. Grey histograms show fluorescence of cells stained with a control antibody. Graphs in the right show the mean ICOS-L fluorescence in cells transfected with WT or four mutant CHO ICOS-L GFP $R_{300}\Delta$ clones. Asterisks (*: $p < 0.05$; **: $p < 0.01$) indicate significant differences of ICOS-L fluorescence between cells incubated with $ICOS^{-}$ cells (red bars) or with $ICOS^{+}$ cells (blue bars), as determined by one-way ANOVA. White bars are data from cells stained with a control antibody. Data from one representative experiment of two experiments performed with similar results

ICOS is taken inside and transferred to $ICOS\text{-}L^{+}$ cells together with its ligand.

4 | DISCUSSION

This study analyzes the mechanisms involved in the fast disappearance of ICOS-L from the surface of APC and other cells expressing ICOS-L upon interaction with ICOS-expressing cells. Available data indicate that a tight control of ICOS-L expression is needed for normal development of immune responses and to prevent autoimmune diseases.[20,34,38–40,56] In B lymphocytes, downmodulation of surface ICOS-L can be induced by interaction with ICOS, and also by PKC, cytokine and antigen signals.[44,45] Surface ICOS-L levels are lower in spleen or bone marrow cells from wild type as compared to cells from ICOS-deficient mice (see i.e.[12,23]). This fact suggests that ICOS-L levels in wild-type mice are maintained low in an ICOS-dependent fashion, even though ICOS expression by T cells is very low under

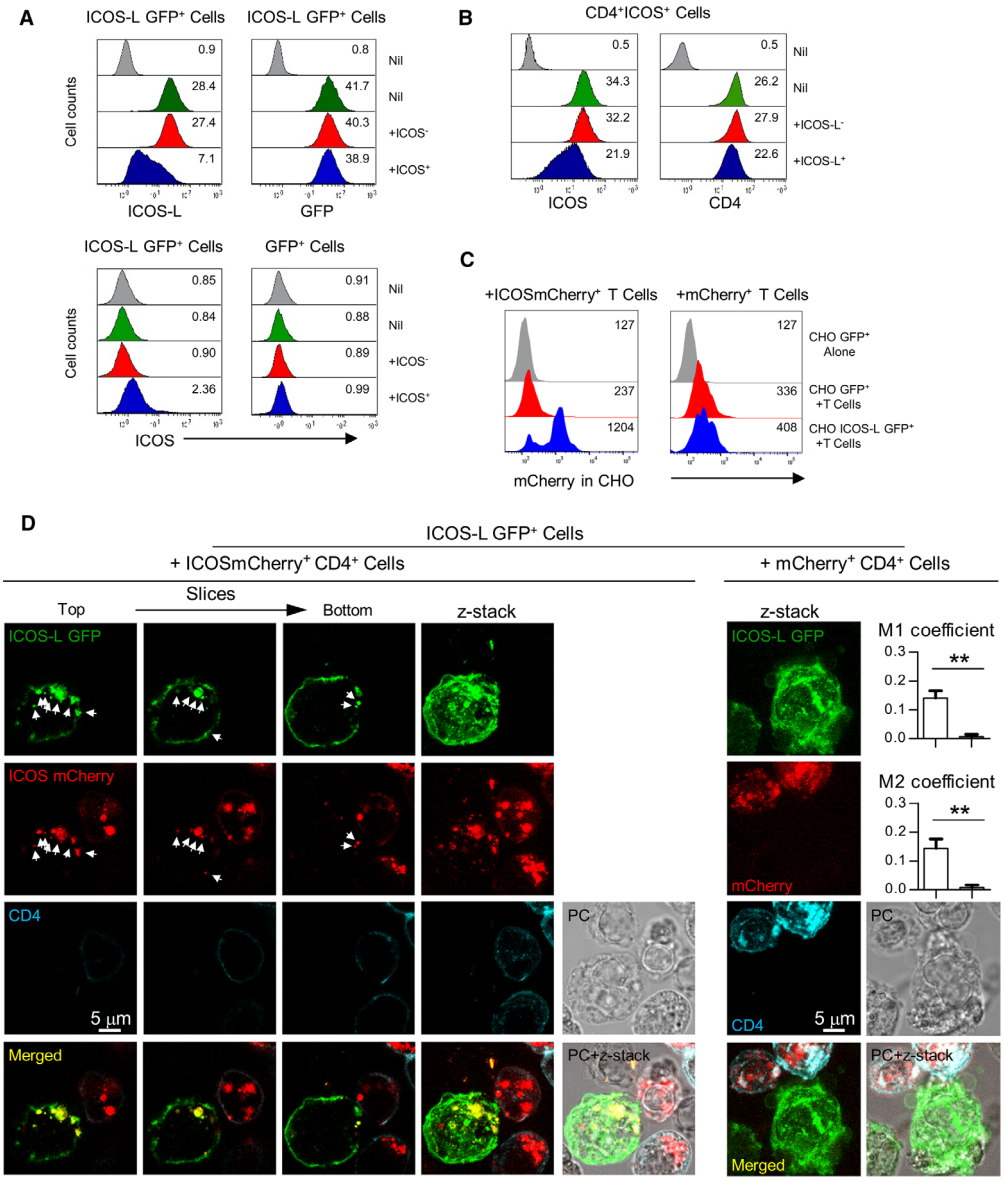

FIGURE 8 **Transfer of ICOS during co-incubation of cells expressing ICOS and ICOS-L.**
(A). CHO cells expressing a fusion protein of GFP and wild type mouse ICOS-L (ICOS-L GFP$^+$ cells) downmodulate surface ICOS-L and express low levels of ICOS when cultured in the presence of ICOS$^+$ T cells. CHO ICOS-L GFP$^+$ cells were incubated at 37°C for 30 min alone (green histograms), with ICOS-deficient T cells (H4$^-$.A5 cells, red histograms), or with ICOS$^+$ T cells (D10 cells, blue histograms), then stained in the cold for surface CD4, ICOS-L, and ICOS, as indicated. Then, the CHO cells (GFP$^+$CD4$^-$ cells) were gated, analyzed for surface ICOS-L, GFP (top panels), or ICOS (lower left). ICOS expression in control CHO GFP transfectants lacking surface ICOS-L (GFP$^+$ cells) in the same conditions is shown (lower right). Histograms of cells stained with control isotype antibodies, or of control GFP$^-$ CHO cells are in grey. **(B).** Cells of the CD4$^+$ ICOS$^+$ D10 cell line (gated as GFP$^-$CD4$^+$ cells) lose surface ICOS when co-incubated for 30 min with ICOS-L GFP$^+$ CHO cells (blue histogram, left panel). This was not observed upon co-incubation with control CHO GFP transfectants (red histogram) or with medium alone (green histogram). In contrast, other T cell surface proteins like CD4 had minor changes in the same conditions (right panel). Histograms in grey show staining with control isotype antibodies. **(C).** CHO cells expressing ICOS-L GFP can incorporate red fluorescence when co-incubated with T cell expressing ICOSmCherry fusion protein (left panel, blue histogram). This is not found in control GFP-expressing cells (left panel, red histogram), or with cells expressing mCherry alone (right panel, blue histogram). Furthermore, red fluorescence is similar in ICOS-L$^+$ (right panel, blue histograms) or ICOS-L$^-$ CHO cells (right panel, red histograms) incubated with control T cell expressing mCherry alone. Grey histograms represent red fluorescence in CHO cells alone. **(D).** Confocal analysis of ICOS-L GFP M12 cells (green) co-incubated with T cell transfectants (CD4$^+$, blue) expressing an ICOSmCherry fusion protein (red) (left panels). ICOS-L GFP is found in the cell membrane and in intracellular vesicles, as shown in distinct z-slices or in combined projection (z-stack). Furthermore, ICOS-L GFP M12 cells incorporate ICOSmCherry, detected as red fluorescence in juxtamembrane or intracellular sites that co-localize with ICOS-L GFP (arrows). This is not observed in ICOS-L GFP M12 cells incubated with control T cell expressing mCherry alone (right panels). Graphs show colocalization quantified as thresholded Manders (M1, M2) coefficients in the presence of T cells expressing ICOSmCherry (white bars) or cells expressing mCherry (grey bars). **: $p < 0.01$, as determined by the Student's t test

steady state conditions "in vivo". Removal of ICOS-L prevents ICOS-mediated costimulatory signals of activated and differentiated ICOS$^+$ T lymphocytes, including Tfh cells.[17,26–28,32–34,56,57] In normal or tumor cells of hematopoietic and non-hematopoietic origin that express ICOS-L, ICOS-L downmodulation would suppress its own signals.[20,30,31,35–37]

In B lymphocytes, ICOS-L downmodulation is induced by interaction with ICOS, by PKC activators, or by anti-IgM antibodies.[45] Interestingly, PKC and anti-IgM induce ICOS-L shedding and release into supernatants, that was dependent on α-secretase activity. In contrast, ICOS-induced ICOS-L downmodulation was not accompanied by efficient ICOS-L shedding, and α-secretase inhibition had a low effect on ICOS-induced downmodulation.[45] In agreement with these data, we find that the α-secretase inhibitor GM6001 had a negligible effect on ICOS-L downmodulation in our system (Table S1). Furthermore, our studies using inhibitors specific for a broad range of proteinase activities confirm that shedding mediated by α-secretase or other proteinases plays a minor role, if any, in early ICOS-induced ICOS-L downmodulation (Table S1).

Our analysis of ICOS-induced reduction of surface ICOS-L show that, instead, there is a fast internalization of ICOS-L, as ICOS-L was readily detected inside the cells after ICOS-L downmodulation, suggesting that it was endocytosed. This seems a physiological phenomenon, as substantial amounts of ICOS-L have been found inside naïve, memory, and germinal center B cells; ICOS-L can be rapidly translocated to the surface during antigen-specific T:B cell interactions in the germinal centers.[58] We examined a number of factors and molecules involved in different modes of endocytosis. From our analysis, it follows that ICOS-L internalization was dependent on temperature and actin cytoskeleton. The effect of inhibitors also indicated a modest role for clathrin- and caveolin-dependent endocytosis. Rather, ICOS-L endocytosis was mainly mediated by mechanisms dependent on the GTPase Dynamin and sensitive to cholesterol depletion. There is growing evidence for different mechanisms of endocytosis that are sensitive to cholesterol depletion and lipid raft integrity, yet some of them are largely independent on clathrin or caveolin but dependent on dynamin.[59,60] A possible role for raft-mediated endocytosis is reinforced by the presence of one Cholesterol Recognition/interaction Amino acid Consensus motif (CRAC, [L/V]-X(1-5)-Y-X(1-5)-[R/K]) in the sequence of mouse ICOS-L. CRAC motifs and their reverse CARC ([R/K]-X(1,5)-Y-X(1,5)-[L/V]) motifs are important to cholesterol-protein interaction and protein location in lipid rafts. There are also CRAC-like and CARC-like sequence motifs that fulfill the same function, but with Phenylalanine or even Tryptophan in the place of Tyrosine.[61,62] A search for these motifs in ICOS-L sequences show that they are present in most transmembrane domains of ICOS-L of mammals and other vertebrates, including human ICOS-L. Furthermore, ICOS-L sequences from many different vertebrate species often contain Cys residues at or close to the transmembrane domain (see pages 3–4 in Supplementary Table S2); acylation (i.e. palmytoilation) of these residues might also contribute to location in lipid rafts.[63] Another factor that might favor ICOS-mediated cell-cell interaction and fast endocytosis is the tendency of ICOS-L to oligomerize in solution or on the cell surface.[54]

Although inhibitors of protein kinase C partially prevented endocytosis, and PKC can bind human ICOS-L and mediate ICOS-L signals,[20] we did not find a clear effect of mutation of cytoplasmic residues involved in PKC recruitment. In fact, complete removal of the cytoplasmic tail of ICOS-L did not block internalization. This, plus partial internalization using fixed ICOS-expressing cells suggested additional, complementary mechanisms in ICOS-induced internalization, that might include trans-endocytosis.

Indeed, we could detect specific transfer of ICOS to ICOS-L-bearing cells upon interaction with ICOS$^+$ cells. This would be an example of trans-endocytosis, or trogocytosis, a phenomenon dependent on actin cytoskeleton reorganization that has a well stablished role in the control of immune processes through cell-cell contact.[64] One case for trans-endocytosis has been described in the CD28- or CTLA-4-mediated transfer of CD80 and CD86 from APC to T cells. In this case, control of CD28 signaling through trogocytosis involves members of both the CD28 and the B7 families.[65,66] Trans-endocytosis also works the other way, namely the transfer of cell surface proteins and other material from T lymphocytes to APC, i.e. by means of "T cell microvilli particles" (TMP). TMP are enriched in molecules including TCR, CD2, or cytokines involved in APC-mediated activation.[67] Interestingly, ICOS ligation induces rapid, antigen-independent spreading of T cells, with actin cytoskeleton reorganization, cell elongation, and formation of lamellipodia- and filopodia-like structures.[14–16,55] So, it is tempting to speculate that ICOS-ICOS-L interactions might induce effects similar to those described for TMP. Concerning the biological consequences of ICOS-ICOS-L modulation from cell surfaces, it can be foreseen that high ICOS levels could have a selective role in some instances. Particularly interesting is the antigen-independent recruitment of T follicular helper (Tfh) cells to germinal centers, a migration that depends on ICOS interaction with ICOS-L expressed by bystander B lymphocytes.[17] In this case, it can be hypothesized that those Tfh lymphocytes with the highest levels of ICOS expression would be better fit for migration.

Further complexity to the regulation of ICOS-ICOS-L interactions is added by the recent discovery of two new proteins that can specifically bind ICOS-L, namely the $\alpha 5\beta 3$ integrin,[68] and osteopontin.[69] These proteins bind ICOS-L at sites distinct from that of ICOS, and their effect on ICOS-induced ICOS-L internalization and signaling deserves further analysis.

5 | CONCLUSIONS

The present study identifies important novel features in the regulation of ICOS-L function through control of cell surface expression. These mechanisms add to transcriptional regulation and shedding, that occur at later moments. Taken together, the data stress the need for a tight control of ICOS-L expression that is essential for the adequate development and regulation of immune responses,[20,34,39,56] for the

control of migration in ICOS-L$^+$ normal or tumor cells, for the differentiation of dendritic cells or osteoclasts[30,31,36,37,69] and normal renal function.[68] So, downmodulation of ICOS-L within minutes by ICOS, or within hours by BCR or IL-4 stimuli, seems necessary to adequate ICOS-L function,[44,45] as is the blocking of ICOS-L modulation in B cells by CD40 signals that contribute to germinal center development.[44,57] Thus, fine-tuning of ICOS-L expression through distinct mechanisms at different moments opens new therapeutic approaches in autoimmune diseases and the control of tumor growth.

DECLARATIONS

Ethics approval and consent to participate

Consent to participate is not applicable.

CONSENT FOR PUBLICATION

Not applicable.

AVAILABILITY OF SUPPORTING DATA AND MATERIALS

Data and materials are available from the corresponding author on reasonable request.

COMPETING INTERESTS

The authors declare that they have no competing interest.

FUNDING

Supported by Grants PI13/01809 (to J.M.R.), PI13/02153 and PI16CIII/00012 (to P.P.) from "Acción Estratégica en Salud, Plan Estatal I+D+i", Ministerio de Economía, Industria y Competitividad (MINECO, Spain) and by the Associazione Italiana Ricerca sul Cancro (Grant IG20714, AIRC, Milan), Fondazione Amici di Jean (Torino), and Fondazione Cariplo (2017-0535) (to U.D.).

AUTHORSHIP

LA-F, MM-C, GO, and LG-P performed experiments and analyzed the data; YA, JY and UD provided essential materials and contributed to manuscript drafts; JMR and PP conceived the study, performed experiments and wrote the manuscript. All authors read and approved the manuscript.

LA-F and MM-C contributed equally to this work.

ACKNOWLEDGEMENTS

The authors thank Dr. O. Zaragoza and the Unidad de Microscopía Electrónica y Confocal, Instituto de Salud Carlos III, for help in confocal microscopy.

REFERENCES

1. Sharpe AH, Freeman GJ. The B7-CD28 superfamily. *Nat Rev Immunol*. 2002;2:116-126.
2. Rudd CE, Schneider H. Unifying concepts in CD28, ICOS and CTLA4 coreceptor signalling. *Nat Rev Immunol*. 2003;3:544-556.
3. Podojil JR, Miller SD. Targeting the B7 family of co-stimulatory molecules: successes and challenges. *BioDrugs*. 2013;27:1-13.
4. Redoglia V, Dianzani U, Rojo JM, et al. Characterization of H4: a murine T lymphocyte activation molecule functionally and physically associated with the CD3/TCR. *Eur J Immunol*. 1996;26:2781-2789.
5. Buonfiglio D, Bragardo M, Bonissoni S, et al. Characterization of a novel human surface molecule selectively expressed by mature thymocytes, activated T cells and subsets of T cell lymphomas. *Eur J Immunol*. 1999;29:2863-2874.
6. Hutloff A, Dittrich AM, Beier KC, et al. ICOS is an inducible T-cell co-stimulator structurally and functionally related to CD28. *Nature*. 1999;397:263-266.
7. Yoshinaga SK, Whoriskey JS, Khare SD, et al. T-cell co-stimulation through B7RP-1 and ICOS. *Nature*. 1999;402:827-832.
8. Grimbacher B, Hutloff A, Schleiser M, et al. Homozygous loss of ICOS is associated with adult-onset common variable immunodeficiency. *Nature Immunol*. 2003;4:261-268.
9. Dong C, Temann U-A, Flavell RA. Critical role of Inducible Costimulator in germinal center reactions. *J Immunol*. 2001;166:3659-3662.
10. Linterman MA, Rigby RJ, Wong RK, et al. Follicular helper T cells are required for systemic autoimmunity. *J Exp Med*. 2009;206:561-576.
11. Yong PFK, Salzer U, Grimbacher B. The role of costimulation in antibody deficiencies: ICOS and common variable immunodeficiency. *Immunol Rev*. 2009;229:101-113.
12. Mittereder N, Kuta E, Bhat G, et al. Loss of immune tolerance is controlled by ICOS in Sle1 mice. *J Immunol*. 2016;197:491-503.
13. Roussel L, Landekic M, Golizeh M, et al. Loss of human ICOSL results in combined immunodeficiency. *J Exp Med*. 2018;215:3151-3164.
14. Franko JL, Levine AD. Antigen-independent adhesion and cell spreading by inducible costimulator engagement inhibits T cell migration in a PI-3K-dependent manner. *J Leukoc Biol*. 2009;85:526-538.
15. Nukada Y, Okamoto N, Konakahara S, et al. AILIM/ICOS-mediated elongation of activated T cells is regulated by both the PI3-kinase/Akt and Rho family cascade. *Int Immunol*. 2006;18:1815-1824.
16. Acosta Y, Zafra M, Ojeda G, et al. Biased binding of class IA phosphatidyl inositol 3-kinase subunits to inducible costimulator (CD278). *Cell Mol Life Sci*. 2011;68:3065-3079.
17. Xu H, Li X, Liu D, et al. Follicular T-helper cell recruitment governed by bystander B cells and ICOS-driven motility. *Nature*. 2013;496:523-527.
18. Burmeister Y, Lischke T, Dahler AC, et al. ICOS controls the pool size of effector-memory and regulatory T cells. *J Immunol*. 2008;180:774-782.
19. Moore TV, Clay BS, Ferreira CM, et al. Protective effector memory CD4 T cells depend on ICOS for survival. *PLoS ONE*. 2011;6:e16529.
20. Hedl M, Lahiri A, Ning K, et al. Pattern Recognition Receptor signaling in human dendritic cells is enhanced by ICOS ligand and modulated by the Crohn's Disease ICOSLG risk allele. *Immunity*. 2014;40:734-746.
21. Mirchandani AS, Besnard A-G, Yip E, et al. Type 2 innate lymphoid cells drive CD4+ Th2 cell responses. *J Immunol*. 2014;192:2442-2448.
22. Maazi H, Patel N, Sankaranarayanan I, et al. ICOS:ICOS-Ligand interaction is required for type 2 Innate Lymphoid Cell function, home-

ostasis, and induction of airway hyperreactivity. *Immunity*. 2015;42:538-551.
23. Montes-Casado M, Ojeda G, Aragoneses-Fenoll L, et al. ICOS deficiency hampers the homeostasis, development and function of NK cells. *PloS ONE*. 2019;14:e0219449.
24. Aicher A, Hayden-Ledbetter M, Brady WA, et al. Characterization of human inducible costimulator ligand expression and function. *J Immunol*. 2000;164:4689-4696.
25. Ling V, Wu PW, Finnerty HF, et al. Identification of GL50, a novel B7-like protein that functionally binds to ICOS receptor. *J Immunol*. 2000;164:1653-1657.
26. Khayyamian S, Hutloff A, Buchner K, et al. ICOS-ligand, expressed on human endothelial cells, costimulates Th1 and Th2 cytokine secretion by memory CD4+ T cells. *Proc Natl Acad Sci USA*. 2002;99:6198-6203.
27. Wahl P, Schoop R, Bilic G, et al. Renal tubular epithelial expression of the costimulatory molecule B7RP-1 (Inducible Costimulator ligand). *J Am Soc Nephrol*. 2002;13:1517-1526.
28. Swallow MM, Wallin JJ, Sha WC. B7h, a novel costimulatory homolog of B7.1 and B7.2, is induced by TNFα. *Immunity*. 1999;11:423-432.
29. Collins M, Ling V, Carreno BM. The B7 family of immune-regulatory ligands. *Genome Biol*. 2005;6:223.
30. Dianzani C, Minelli R, Gigliotti CL, et al. B7h triggering inhibits the migration of tumor cell lines. *J Immunol*. 2014;192:4921-4931.
31. Dianzani C, Minelli R, Mesturini R, et al. B7h triggering inhibits umbilical vascular endothelial cell adhesiveness to colon carcinoma cell lines and polymorphonuclear cells. *J Immunol*. 2010;185:3970-3979.
32. Wang S, Zhu G, Chapoval AI, et al. Costimulation of T cells by B7-H2, A B7-like molecule that binds ICOS. *Blood*. 2000;96:2808-2813.
33. Guo J, Stolina M, Bready JV, et al. Stimulatory effects of B7-related protein-1 on cellular and humoral immune responses in mice. *J Immunol*. 2001;166:5578-5584.
34. Nurieva RI, Mai XM, Forbush K, et al. B7h is required for T cell activation, differentiation, and effector function. *Proc Natl Acad Sci USA*. 2003;100:14163-14168.
35. Tang G, Qin Q, Zhang P, et al. Reverse signaling using an inducible costimulator to enhance immunogenic function of dendritic cells. *Cell Mol Life Sci*. 2009;66:3067-3080.
36. Occhipinti S, Dianzani C, Chiocchetti A, et al. Triggering of B7h by the ICOS modulates maturation and migration of monocyte-derived Dendritic Cells. *J Immunol*. 2013;190:1125-1134.
37. Gigliotti CL, Boggio E, Clemente N, et al. ICOS-Ligand triggering impairs osteoclast differentiation and function in vitro and in vivo. *J Immunol*. 2016;197:3905-3916.
38. Pratama A, Srivastava M, Williams NJ, et al. MicroRNA-146a regulates ICOS–ICOSL signalling to limit accumulation of T follicular helper cells and germinal centres. *Nat Commun*. 2015;6:6436.
39. Teichmann LL, Cullen JL, Kashgarian M, et al. Local triggering of the ICOS coreceptor by CD11c+ myeloid cells drives organ inflammation in Lupus. *Immunity*. 2015;42:552-565.
40. Lownik JC, Luker AJ, Damle SR, et al. ADAM10-mediated ICOS Ligand shedding on B cells is necessary for proper T cell ICOS regulation and T follicular helper responses. *J Immunol*. 2017;199:2305-2315.
41. Lownik JC, Wimberly JL, Conrad DH, et al. B Cell ADAM10 controls murine lupus progression through regulation of the ICOS:ICOS Ligand axis. *J Immunol*. 2019;202:664-674.
42. Watanabe M, Takagi Y, Kotani M, et al. Down-regulation of ICOS ligand by interaction with ICOS functions as a regulatory mechanism for immune responses. *J Immunol*. 2008;180:5222-5234.
43. Sato T, Kanai T, Watanabe M, et al. Hyperexpression of inducible costimulator and its contribution on lamina propria T cells in inflammatory bowel disease. *Gastroenterology*. 2004;126:829-839.
44. Liang L, Porter EM, Sha WC. Constitutive expression of the B7h ligand for Inducible Costimulator on naive B cells is extinguished after activation by distinct B cell receptor and Interleukin 4 receptor-mediated pathways and can be rescued by CD40 signaling. *J Exp Med*. 2002;196:97-108.
45. Logue EC, Bakkour S, Murphy MM, et al. ICOS-induced B7h shedding on B cells is inhibited by TLR7/8 and TLR9. *J Immunol*. 2006;177:2356-2364.
46. Marczynska J, Ozga A, Wlodarczyk A, et al. The role of metalloproteinase ADAM17 in regulating ICOS Ligand–mediated humoral immune responses. *J Immunol*. 2014;193:2753-2763.
47. Feito MJ, Vaschetto R, Criado G, et al. Mechanisms of H4/ICOS costimulation: effects on proximal TCR signals and MAP kinase pathways. *Eur J Immunol*. 2003;33:204-214.
48. Cohn LE, Glimcher LH, Waldmann RA, et al. Identification of functional regions on the I-Ab molecule by site-directed mutagenesis. *Proc Natl Acad Sci USA*. 1986;83:747-751.
49. Díez-Orejas R, Ballester S, Feito MJ, et al. Genetic and immunochemical evidence for CD4-dependent association of p56lck with the α;β; T-cell receptor (TCR): regulation of TCR-induced activation. *EMBO J*. 1994;13:90-99.
50. Ojeda G, Ronda M, Ballester S, et al. A hyperreactive variant of a CD4+ T cell line is activated by syngeneic antigen presenting cells in the absence of antigen. *Cell Immunol*. 1995;164:265-278.
51. Rojo JM, Pini E, Ojeda G, et al. CD4+ICOS+ T lymphocytes inhibit T cell activation 'in vitro' and attenuate autoimmune encephalitis 'in vivo. *Int Immunol*. 2008;20:577-589.
52. Darlington PJ, Baroja ML, Chau TA, et al. Surface cytotoxic T lymphocyte-associated antigen 4 partitions within lipìd rafts and relocates to the immunological synapse under conditions of inhibition of T cell activation. *J Exp Med*. 2002;195:1337-1347.
53. Jiménez-Periañez A, Ojeda G, Criado G, et al. Complement regulatory protein Crry/p65-mediated signalling in T lymphocytes: role of its cytoplasmic domain and partitioning into lipid rafts. *J Leukoc Biol*. 2005;78:1386-1396.
54. Chattopadhyay K, Bhatia S, Fiser A, et al. Structural basis of Inducible Costimulator Ligand costimulatory function: determination of the cell surface oligomeric state and functional mapping of the receptor binding site of the protein. *J Immunol*. 2006;177:3920-3929.
55. Acosta YY, Ojeda G, Zafra MP, et al. Dissociation of actin polymerization and lipid raft accumulation by ligation of the Inducible Costimulator (ICOS, CD278). *Inmunología*. 2012;31:4-12.
56. Ara G, Baher A, Storm N, et al. Potent activity of soluble B7RP-1-Fc in therapy of murine tumors in syngeneic hosts. *Int J Cancer*. 2003;103:501-507.
57. Liu D, Xu H, Shih C, et al. T-B-cell entanglement and ICOSL-driven feed-forward regulation of germinal centre reaction. *Nature*. 2015;517:214-218.
58. Papa I, Saliba D, Ponzoni M, et al. TFH-derived dopamine accelerates productive synapses in germinal centres. *Nature*. 2017;547:318-323.
59. Mayor S, Pagano RE. Pathways of clathrin-independent endocytosis. *Nat Rev Mol Cell Biol*. 2007;8:603-612.
60. Lajoie P, Nabi IR. Lipid rafts, caveolae, and their endocytosis. *Int Rev Cell Mol Biol*. 2010;282:135-163.
61. Fantini J, Barrantes FJ. How cholesterol interacts with membrane proteins: an exploration of cholesterol-binding sites including CRAC, CARC, and tilted domains. *Front Physiol*. 2013;4:31.
62. Listowski MA, Leluk J, Kraszewski S, et al. Cholesterol interaction with the MAGUK protein family member, MPP1, via CRAC and CRAC-like motifs: an in silico docking analysis. *PLoS ONE*. 2015;10:e0133141.
63. Chamberlain LH, Shipston MJ. The physiology of protein S-acylation. *Physiol Rev*. 2015;95:341-376.
64. Davis DM. Intercellular transfer of cell-surface proteins is common and can affect many stages of an immune response. *Nat Rev Immunol*. 2007;7:238-243.
65. Hwang I, Huang J-F, Kishimoto H, et al. T cells can use either T cell receptor or CD28 receptors to absorb and internalize cell

surface molecules derived from antigen-presenting cells. *J Exp Med*. 2000;191:1137-1148.
66. Qureshi OS, Zheng Y, Nakamura K, et al. Trans-endocytosis of CD80 and CD86: a molecular basis for the cell-extrinsic function of CTLA-4. *Science*. 2011;332:600-603.
67. Kim H-R, Mun Y, Lee K-S, et al. T cell microvilli constitute immunological synaptosomes that carry messages to antigen-presenting cells. *Nat Commun*. 2018;9:3630.
68. Koh KH, Cao Y, Mangos S, et al. Nonimmune cell-derived ICOS ligand functions as a renoprotective $\alpha v\beta 3$ integrin-selective antagonist. *J Clin Invest*. 2019;129:1713-1726.
69. Raineri D, Dianzani C, Cappellano G, et al. Osteopontin binds ICOSL promoting tumor metastasis. *Commun Biol*. 2020;3:615.

SUPPORTING INFORMATION

Additional information may be found online in the Supporting Information section at the end of the article.

How to cite this article: Aragoneses-Fenoll L, Montes-Casado M, Ojeda G et al. Role of endocytosis and trans-endocytosis in ICOS costimulator-induced downmodulation of the ICOS Ligand. *J Leukoc Biol*. 2021;1-18. https://doi.org/10.1002/JLB.2A0220-127R